

Formation of metal-nicotianamine complexes as affected by pH, ligand exchange with citrate and metal exchange. A study by electrospray ionization time-of-flight mass spectrometry

Rubén Rellán-Álvarez, Javier Abadía and Ana Álvarez-Fernández*

Department of Plant Nutrition, Aula Dei Experimental Station (CSIC), P.O. Box 202, 50080 Zaragoza, Spain

Received 16 October 2007; Revised 18 February 2008; Accepted 3 March 2008

Nicotianamine (NA) is considered as a key element in plant metal homeostasis. This non-proteinogenic amino acid has an optimal structure for chelation of metal ions, with six functional groups that allow octahedral coordination. The ability to chelate metals by NA is largely dependent on the pK of the resulting complex and the pH of the solution, with most metals being chelated at neutral or basic pH values. *In silico* calculations using pKa and pK values have predicted the occurrence of metal-NA complexes in plant fluids, but the use of soft ionization techniques (e.g. electrospray), together with high-resolution mass spectrometers (e.g. time-of-flight mass detector), can offer direct and metal-specific information on the speciation of NA in solution. We have used direct infusion electrospray ionization mass spectrometry (time-of-flight) ESI-MS(TOF) to study the complexation of Mn, Fe(II), Fe(III), Ni, Cu by NA. The pH dependence of the metal-NA complexes in ESI-MS was compared to that predicted *in silico*. Possible exchange reactions that may occur between Fe-NA and other metal micronutrients as Zn and Cu, as well as between Fe-NA and citrate, another possible Fe ligand candidate in plants, were studied at pH 5.5 and 7.5, values typical of the plant xylem and phloem saps. Metal-NA complexes were generally observed in the ESI-MS experiments at a pH value approximately 1–2 units lower than that predicted *in silico*, and this difference could be only partially explained by the estimated error, approximately 0.3 pH units, associated with measuring pH in organic solvent-containing solutions. Iron-NA complexes are less likely to participate in ligand- and metal-exchange reactions at pH 7.5 than at pH 5.5. Results support that NA may be the ligand chelating Fe at pH values usually found in phloem sap, whereas in the xylem sap NA is not likely to be involved in Fe transport, conversely to what occurs with other metals such as Cu and Ni. Some considerations that need to be addressed when studying metal complexes in plant compartments by ESI-MS are also discussed. Copyright © 2008 John Wiley & Sons, Ltd.

Metals such as Mn, Fe, Ni, Cu or Zn are essential for plants, since they participate in numerous metabolic processes in different plant tissues and cell compartments. When these metals are in short supply, plants show deficiency symptoms such as growth reduction and reduced photosynthesis. However, when metals are in excess oxidative stress and other cellular disturbances occur, and plants develop toxicity symptoms.¹ For these reasons, the processes involved in metal acquisition by roots and transport to the different plant organs must be tightly regulated, so that metals can be available where they are needed and in an appropriate

chemical form. The tendency toward a relatively stable equilibrium between these interdependent mechanisms, maintained by physiological processes, is usually called metal homeostasis.

A key element in plant metal homeostasis is the non-proteinogenic amino acid nicotianamine (NA), first discovered by Noma *et al.*² Nicotianamine has an optimal structure for chelation of metal ions, with six functional groups that allow octahedral coordination, the distances between functional groups being optimal for the formation of chelate rings. Nicotianamine is known to chelate many metals, including Fe(II) and Fe(III),^{3,4} Mn(II), Co(II), Ni(II), Cu(II) and Zn(II).^{5,6} The NA stability constants (log K) of the metal-NA complexes with Fe(III), Cu(II), Ni(II), Zn(II), Fe(II) and Mn(II) are 20.6, 18.6, 16.1, 15.4, 12.8 and 8.8, respectively.^{3,4,6}

Nicotianamine is thought to be important in the speciation of soluble Fe in different plant compartments,⁷ because it is

*Correspondence to: A. Álvarez-Fernández, Department of Plant Nutrition, Aula Dei Experimental Station (CSIC), P.O. Box 202, 50080 Zaragoza, Spain.

E-mail: ana.alvarez@eead.csic.es

Contract/grant sponsor: Spanish Ministry of Education and Science (MEC; co-financed with FEDER); contract/grant number: AGL2006-1416 and AGL2007-61948.

able to form stable complexes with both Fe(II) and Fe(III) at neutral and weakly alkaline pH values.⁸ Although the Fe(III)-NA complex has a much higher stability constant, the Fe(II)-NA complex is also kinetically stable under aerobic conditions.³ Nicotianamine appears to be ubiquitous in higher plants and is present in all tissues.⁹ For instance, NA concentrations are relatively increased in root tips of sunflower and barley in the regions of main uptake and radial transport of Fe.¹⁰ Also, both Fe-NA complexes constitute non-toxic Fe pools, because they are relatively poor Fenton reagents.³ In the NA-lacking tomato mutant *chloronerva*, enhanced activities of antioxidant enzymes¹¹ and precipitation of Fe in vacuoles and mitochondria¹² do occur.

The possible roles of NA in long-distance metal transport, both in the xylem and phloem compartments, is still being explored. Nicotianamine has been observed in the xylem at μM concentrations¹³ although it does not seem to be absolutely necessary for xylem metal transport. For instance, in the NA-deficient tomato mutant *chloronerva*, Fe, Mn and Zn accumulate in old leaves.¹⁴ Instead, Fe is thought to be transported through the xylem complexed with citrate.^{15,16} Recent findings support that the FRD3 protein transporter could import citrate into the root vasculature, and *frd3* mutants show symptoms of Fe deficiency that could be alleviated by external citrate supply.¹⁷ In young leaves, Fe-ligand exchange (from citrate to NA) could occur during Fe transfer from xylem to phloem, and Fe-NA could pass through membranes by metal-NA complex specific transporters, as suggested by Takahashi *et al.*¹³ Nicotianamine has been observed in the phloem, and could be involved in Fe phloem loading and unloading, although a 17 kD polypeptide has been proposed to be the Fe carrier in the phloem of *Ricinus*.^{18–20} After the cloning of nicotianamine synthase (NAS) new tools are available to modulate the concentrations of NA in different plant tissues.^{21–23} Nicotianamine involvement in long-distance transport is also supported by the fact that the protein OsYLS2, which can transport Fe(II)-NA and Mn(II)-NA complexes, is expressed in phloem companion cells of rice leaves.²⁴ The protein ZmYS1, which transports both Fe(II)-NA²⁵ and Fe(III)-NA,^{25,26} is able to rescue Fe-deficient yeast mutants and also transports Fe-NA complexes when expressed in *Xenopus* oocytes. In addition to its role in long-distance metal transport, NA might be involved in the regulation of intercellular metal transfer.¹³ Also, higher concentrations of NA are required for flower and seed development than for leaf development.¹³

Nicotianamine can also form complexes with other metals apart from Fe. For instance, from *in silico* studies it has been proposed that Cu xylem transport could rely on complexation with NA.³ In fact, the Cu concentration in the xylem of the NA-deficient tomato mutant *chloronerva* was enhanced by NA application, and a high supply of Cu resulted in higher NA concentration.²⁷ It seems also clear that NA is involved in Ni tolerance and hyper-accumulation. Vacchina *et al.*²⁸ identified the Ni(II)-NA complex in the Ni hyper-accumulator species *Thlaspi caerulescens*. Also, a high NAS expression was found by microarray analysis in the hyper-accumulator species *Arabidopsis halleri*.²⁹ Transgenic plants over-expressing NAS have been constructed and proved to be tolerant to high Ni

concentrations, most likely due to the higher constitutive levels of NA.^{30–32}

Until now, a large part of the current knowledge on the role of metal-NA complexes in micronutrient plant nutrition has been gained using either indirect measurements or *in silico* calculations.³ Further investigation in this area should include direct determination of the possible metal-NA complexes, as suggested by Hider *et al.*³³ Recent examples of this approach were the determination of the Ni(II)-NA complex in the Ni hyper-accumulator *T. caerulescens* by mass spectrometry,^{28,34} the identification of different metal-phytosiderophores by zwitterionic hydrophilic interaction liquid chromatography (ZIC-HILIC) coupled to ESI-MS,³⁵ and the characterization of Fe(II)/(III)-phytosiderophore complexes by direct infusion nano-ESI-Fourier transform ion cyclotron resonance MS.³⁶

The aim of our work was to study the complexation of Mn(II), Fe(II), Fe(III), Ni(II), Cu(II), Zn(II) and Cd(II) by NA, using ESI-TOF(MS) at different pH conditions and comparing the results with *in silico* estimations. Specifically, the formation of Fe(II)-NA and Fe(III)-NA complexes was analyzed in detail, by studying ligand-exchange reactions with citrate as well as metal-exchange reactions with Zn and Cu. These studies were carried out using typical xylem and phloem pH values, in an effort to gain a better insight into the possible roles of NA in long-distance metal transport in plants.

EXPERIMENTAL

Chemicals

All buffers and standard solutions were prepared with LC/MS grade water (Riedel-de Hën, Seelze, Germany). Ammonium bicarbonate (99.5%, Fluka), ammonium acetate (99.99%, Aldrich), leucine-enkephaline (Tyr-Gly-Gly-Phe-Leu, 98%, Sigma), methionine (99%, Sigma), citric acid (99%, Sigma), formic acid (50%, Fluka), acetonitrile and 2-propanol (in both cases LC/MS grade, Riedel-de Hën) were purchased from Sigma (St. Louis, MO, USA). Iron(II) chloride (98%, Aldrich), Ni(II) chloride (99.9%, Sigma) and Cd(II) chloride (98%, Sigma) were also purchased from Sigma. Manganese(II), Fe(III), Cu(II) and Zn(II) were Titrisol[®] metal standards (1 g of metal in 15% HCl, Merck, Darmstadt, Germany). Glutathione (99%) and nicotianamine (98%) were purchased from Calbiochem (San Diego, CA, USA) and T. Hasegawa Co., Ltd. (Kawasaki, Japan), respectively.

Preparation of standard solutions

Solutions for tuning the mass spectrometer were (1) 10 mM LiOH, 0.2% (v/v) formic acid and 50% (v/v) 2-propanol, and (2) 1 μM leucine-enkephaline, 20 μM methionine, 5 μM glutathione, 0.1% (v/v) formic acid and 50% (v/v) 2-propanol. Stock solutions of 100 mM ammonium acetate, 100 mM ammonium bicarbonate, 1 mM metal, 1 mM NA and 1 mM citric acid were prepared by dissolving or diluting the starting products in water.

The ESI-TOF mass spectra of Mn(II)-NA, Fe(II)-NA, Fe(III)-NA, Ni(II)-NA, Cu(II)-NA, Zn(II)-NA and Cd(II)-NA were obtained by adding 1 mM NA solutions over 100 mM ammonium bicarbonate, pH 7.1, and then adding the 1 mM

metal standard. Just before ESI-MS(TOF) analysis, samples were diluted with 50% acetonitrile and the pH was measured again and if necessary readjusted with NH_4OH or HCl . A Biotrode[®] pH microelectrode with Idrolyte[®] electrolyte (Metrohm, Herisau, Switzerland), which allows measurements in the presence of organic solvents, was used. The final solution contained 50 μM concentrations of both NA and metal. All possible precautions in the preparation of metal-containing solutions were taken, specially with Fe(II) solutions, including N_2 bubbling, protection from light and immediate analysis to avoid oxidation of Fe(II).

In order to study the effects of pH on the formation of metal-NA complexes, solutions of Mn(II)-NA, Fe(II)-NA, Fe(III)-NA, Ni(II)-NA, Cu(II)-NA, Zn(II)-NA and Cd(II)-NA were prepared at different pH values (2.5 to 8.5) by adding 1 mM NA solutions over 100 mM ammonium acetate (when pH values were lower than 7.0) or ammonium bicarbonate (when pH was higher than 7.0), and then adding the 1 mM metal standard. Just before ESI-MS(TOF) analysis, samples were diluted with 50% acetonitrile and the pH was measured again. The final solution contained 50 μM concentrations of both NA and metal.

Ligand-exchange experiments were carried out with 50 μM solutions of Fe(II)-NA, Fe(III)-NA and citric acid prepared in 50% acetonitrile. Metal-exchange experiments were carried out with 50 μM solutions of Fe(II)-NA, Cu(II) and Zn(II) prepared in 50% acetonitrile. Iron(II)-NA and Fe(III)-NA solutions were buffered at pH values 5.5 and 7.5 as described above.

ESI-MS(TOF) analysis

Analyses were carried out with a BioTOF[®] II (Bruker Daltonics, Billerica, MA, USA) coaxial multipass time-of-flight mass spectrometer (MS(TOF)) equipped with an Apollo electrospray ionization (ESI) source. The maximum resolution of the mass spectrometer detector used is 10 000 FWHM (full width at half-maximum height).

The BioTOF[®] II was operated with endplate and spray tip potentials of 2.8 kV and 3.3 kV, respectively, in negative ion mode, and of 3.0 kV and 3.5 kV, respectively, in positive ion mode. Drying (N_2) and nebulizer gas (N_2) pressures were kept at 30 psi. The mass axis was calibrated using Li-formate adducts in negative ion mode and a mixture of 1 μM leucine-enkephaline, 20 μM methionine and 5 μM glutathione in positive ion mode. Spectra were acquired in the mass/charge ratio (m/z) range of 100–700.

A syringe pump (Cole-Parmer Instruments, Vernon Hills, IL, USA) operated at 4 $\mu\text{L}/\text{min}$ was used to introduce into the ESI chamber the solutions containing metal-NA complexes at different pH values. For ligand-exchange experiments, two syringe pumps operating at 4 $\mu\text{L}/\text{min}^{-1}$ were used, the first containing 50 μM Fe(II)-NA (or Fe(III)-NA) solution and the second containing 50 μM citric acid. Both syringes were connected with a tee to the ESI chamber. The syringe containing Fe-NA was run until a stable $[\text{M}-\text{H}]^{-1}$ signal was obtained. Then, the syringe containing citric acid was switched on and both syringes were run until stabilization of the signal. For metal-exchange experiments, the same set-up was used loading 50 μM Fe(II)-NA in the first syringe and 50 μM Cu(II) or Zn(II) in the second. A thorough

mixing between the content of the two syringes was obtained by using a micro-static mixing PEEK[®] tee (internal swept volume 0.95 μL ; reference M-540A, Upchurch, Oak Harbor, WA, USA) that creates a turbulent flow. Then, the fluid was directed to the ESI chamber (at a flow rate of 8 $\mu\text{L}/\text{min}$) through PEEK[®] tubing (0.127 mm i.d., 250 mm in length, reference 1535, Upchurch). Therefore, the mixture was left to react for 0.5 min before entrance into the ESI chamber.

The system was controlled with the software package BioTOF (version 2.2, Bruker Daltonics). Data were processed with Data Analysis software (version 3.2, Bruker Daltonik GmbH, Bremen, Germany).

Speciation modelling

MINTEQA2 for Windows (version 1.50, Allison Geoscience Consultants, Flowery Branch, GA, USA and HydroGeoLogic, Inc., Herndon, VA, USA) was used to carry out ligand and metal speciation in solutions. All thermodynamic database equilibrium constants were determined in water. Input parameters were metal and ligand concentrations and pH values. NA protonation constants and stability constants for metal-NA complexes were taken from Benes *et al.*⁴ and von Wirén *et al.*³ Citrate protonation constants and stability constants for metal-citrate complexes were taken from Martell and Smith.³⁷

RESULTS AND DISCUSSION

Electrospray ionization of NA and metal-NA complexes

Negative mass spectra of NA and different metal-NA complex solutions at pH 7.1 are shown in Figs. 1 and 2. Nicotianamine showed a major peak corresponding to the monoisotopic $[\text{M}-\text{H}]^{-1}$ ion at an m/z value of 302.1 (Fig. 1(A)). For all metal-NA complexes analyzed, the only metal-NA species observed were singly charged species with 1:1 metal/NA stoichiometry. Major peaks corresponding to the signal of the metal isotope $[\text{M}-\text{H}]^{-1}$ ions were observed at m/z values of 355.1 for ⁵⁵Mn(II)-NA (Fig. 1(B)), 356.1 for ⁵⁶Fe(II)-NA (Fig. 1(C)), 358.1 for ⁵⁸Ni(II)-NA (Fig. 1(E)), 363.1 for ⁶³Cu(II)-NA (Fig. 1(F)), 364.0 for ⁶⁴Zn(II)-NA (Fig. 1(G)), and 414.0 for ¹¹⁴Cd(II)-NA (Fig. 1(H)). Since Fe(III) forms a neutral charge complex with NA, the $[\text{M}-\text{H}]^{-1}$ ion (m/z 355.2) was poorly ionized when compared with the $[\text{M}-\text{H}]^{-1}$ ion of negatively charged divalent metal-NA complexes. Major peaks found in the mass spectrum of Fe(III)-NA (Fig. 1(D)) were at m/z values of 356.2 and 311.2, and could be assigned to the $[\text{M}-\text{H}]^{-1}$ and $[\text{Fe}(\text{II})\text{NA}-\text{H}-\text{CO}_2]^{-1}$ ions of ⁵⁶Fe(II)-NA, respectively. The peak at m/z value of 356.2 indicates that the complex Fe(III)-NA undergoes a reduction to Fe(II)-NA that was apparent in all tested ionization conditions, reaching a minimum at a capillary exit voltage of 40 V (Fig. I in the Supplementary material). Although this reduction is not expected when considering the redox potentials,³⁸ redox reactions have been reported to occur in the ESI process, with reduction being more likely in the negative mode.³⁹ An alteration of the oxidation state of Fe-NA complexes was also found under nano-ESI conditions,³⁶ although in that case it was possible to optimize ionization conditions to eliminate Fe oxidation state changes.

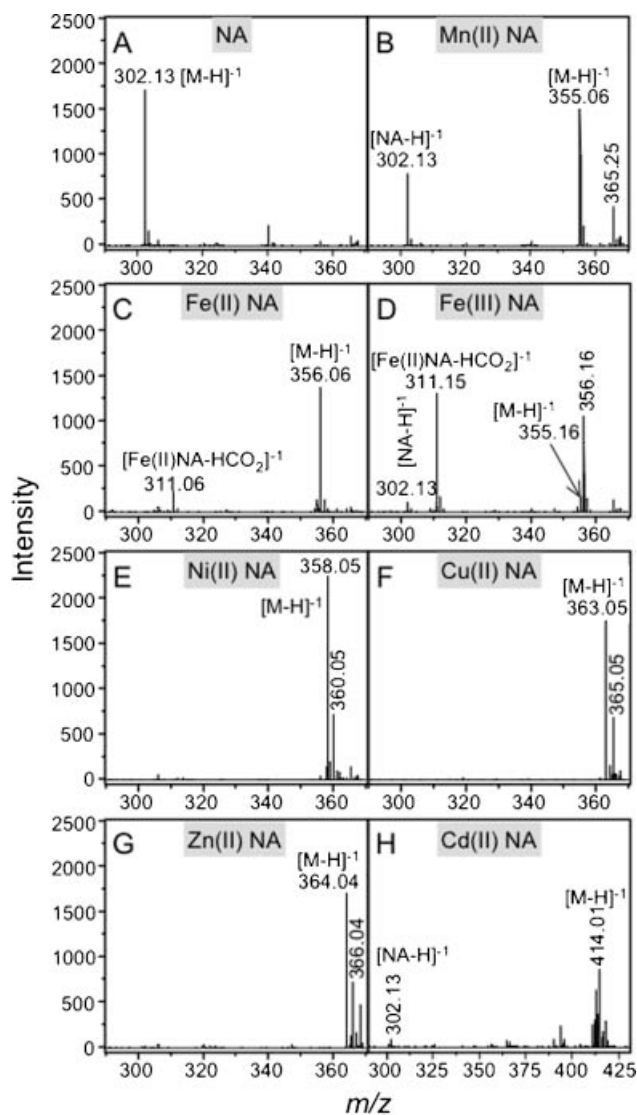


Figure 1. ESI-TOF mass spectra of nicotianamine (A) and the nicotianamine complexes with Mn(II) (B), Fe(II) (C), Fe(III) (D), Ni(II) (E), Cu(II) (F), Zn(II) (G), and Cd(II) (F), in negative ion mode. Data were acquired by injecting 50 μ M solutions of each analyte in 50 mM ammonium acetate, pH 7.1, and 50% acetonitrile.

The peak at m/z value of 311.2 indicates a reduction and concomitant decarboxylation of Fe(III)-NA. Metal reduction reactions followed by a ligand decarboxylation of metal complexes with the concomitant oxidation of amino ($-N-$) to imino N ($-N=$) have also been documented in the literature.⁴⁰ The signal attributed to the $[Fe(II)NA-H-CO_2]^{-1}$ ion was also found in the Fe(II)-NA spectrum (Fig. 1(C)), although with much lower intensity than in the case of Fe(III)-NA (Fig. 1(D)). Another minor signal at m/z 355.1 corresponding to the monoisotopic $[M-H]^{-1}$ ion of Fe(III)-NA was also found in the Fe(II)-NA spectrum (Fig. 1(C)). Oxidation of Fe(II) species could occur during the ESI process and/or the solution preparation. However, oxidation reactions are unlikely to occur during ESI in negative mode, whereas Fe(II) species are easily oxidized by dissolved oxygen, light, etc., during the solution preparation. Presence of Fe(III)-NA in Fe(II)-NA solutions has been observed previously.³⁶ A

minor peak at m/z 302.1 corresponding to the monoisotopic $[M-H]^{-1}$ ion of NA was also found in Mn(II)-NA, suggesting that complexation of Mn with NA was not fully complete at the pH value of 7.1 used in this experiment. A minor signal at m/z 302.1 was also found in the MS spectra of Fe(III)-NA and Cd(II)-NA.

The negative mass spectra were zoomed close to the major signals (Fig. 2) to show in detail the isotopic signatures of the main $[M-H]^{-1}$ ions found. Observed isotopic signatures (Figs. 2(A)–2(D)) matched the theoretical ones (2a–2d). Metal isotopic signatures (insets in Fig. 2) were well preserved in metal-NA complexes, confirming the possibility to use isotopic signatures to identify metal-NA complexes in real samples.

Positive mass spectra (not shown) showed major peaks at m/z values of 304.1, 357.1, 358.1, 360.1, 365.1, 366.1 and 416.0, corresponding to the $[M+H]^{+1}$ ions of NA, ⁵⁵Mn(II)-NA, ⁵⁶Fe(II)-NA, ⁵⁸Ni(II)-NA, ⁶³Cu(II)-NA, ⁶⁴Zn(II)-NA and ¹¹⁴Cd(II)-NA, respectively. The mass spectrum of Fe(III)-NA showed two major peaks at m/z values of 357.0, 358.0 and 313.0, corresponding to the $[Fe(III)NA+H]^{+1}$, $[Fe(II)NA+2H]^{+1}$ and $[Fe(II)NA-CO_2+H]^{+1}$ ions of Fe(II)-NA, respectively.

The effects of capillary cone voltages (20–200 V) and drying gas temperatures (150, 200 and 250°C) on the ionization of NA and metal-NA complexes were studied in negative and positive ion mode (considering the $[M-H]^{-1}$ and $[M+H]^{+1}$ signals, respectively; see Fig. 1 in the Supplementary Material). Both NA and metal-NA complex ionization did not depend on the drying gas temperature at any of the tested capillary cone voltages. The capillary cone voltage, however, had an important effect on the ionization of the analytes. Signal intensity generally reached a maximum around 120 V and did not change with higher voltage values, regardless of the polarity. However, the ionization of the NA and Cu(II)-NA $[M-H]^{-1}$ ions reached a maximum intensity at approximately 90 V, and decreased sharply at higher voltage values. Cleaner spectra were obtained in negative than in positive mode, since in the latter case several unknown signals (artifacts or traces of impurities) with quite large intensities were observed. Signal intensities were not significantly different between both polarity modes, as it could be expected from the zwitterionic character of the NA molecule, which has carboxyl and amino groups that can be easily ionized in negative and positive mode, respectively. Polarity affected markedly Mn(II)-NA ionization, which was similar to that of other metal-NA complexes studied in negative ion mode, whereas in positive ion mode a poorer ionization was observed.

Therefore, the optimal operating conditions chosen included negative ion mode, drying gas temperature of 200°C and capillary cone voltage of 120 V, except for NA and Cu(II)-NA, where a voltage of 90 V was used. Under these conditions, Ni(II)-NA showed the highest intensity. Since all these compounds are in low concentrations in real plant samples, highly sensitive MS devices would be required. In fact, the good ionization of the Ni(II)-NA complex, together with the use of plant Ni hyper-accumulators, could explain why this metal-NA complex has received more attention than others.^{28,34,41,42} Theoretical and experimental m/z values

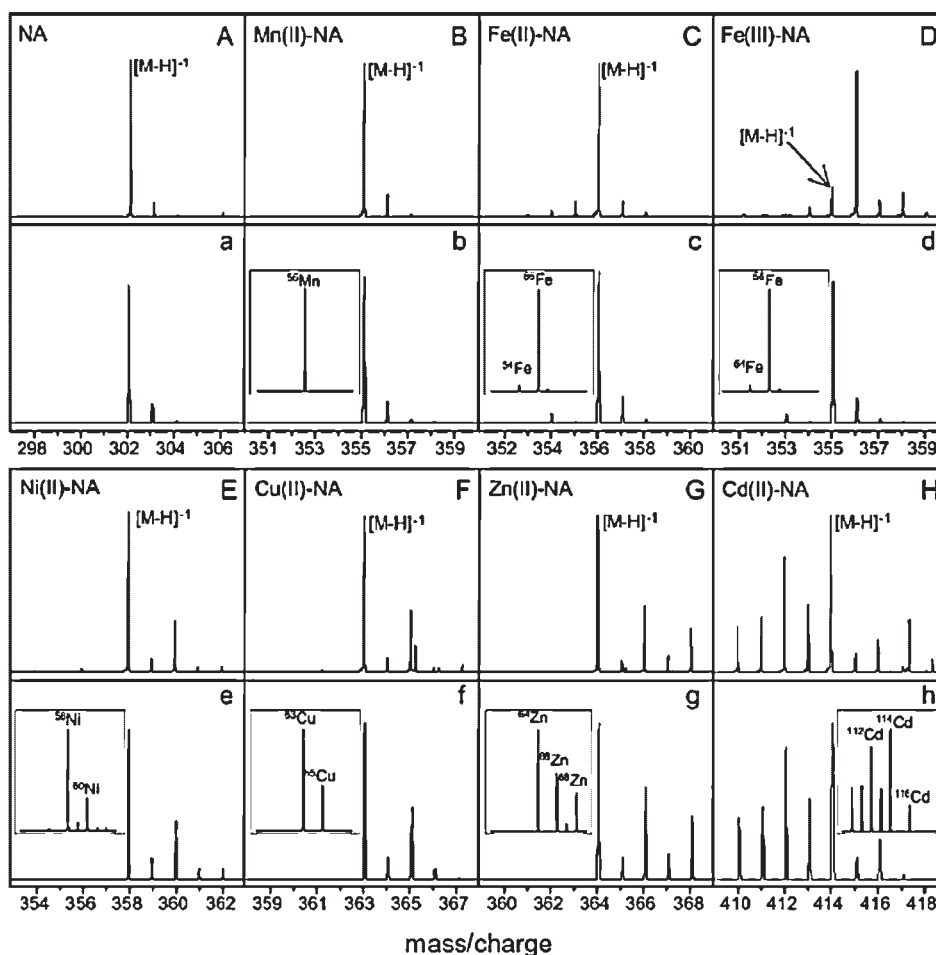


Figure 2. Experimental (upper case letters) and calculated (lower case) zoomed ESI-TOF mass spectra of nicotianamine (A, a) and the nicotianamine complexes with Mn(II) (B, b), Fe(II) (C, c), Fe(III) (D, d), Ni(II) (E, e), Cu(II) (F, f), Zn(II) (G, g), and Cd(II) (H, h) in negative ion mode. Experimental spectra are zoomed from those in Fig. 1. Insets in the calculated mass spectra show the theoretical isotopic distribution of the corresponding metal.

for the most abundant isotopes of each compound described above are shown in Table I of the Supplementary Material. Mass accuracy mean values, using external calibration, were approximately 15 ± 10 ppm (mean ± 3 SD) in negative mode and 13 ± 7 ppm in positive mode.

Effect of pH on metal-NA complexes

The pH dependence of metal-NA complexes was studied by ESI-MS in the pH range from approximately 2.5 to 8.5 (Fig. 3). Results shown are intensities corresponding to the most abundant ions of NA and metal-NA complexes (Figs. 3(A)–3(F)). To assess the metal-NA complex pH dependence, both the NA and metal-NA complex signals must be used, because changes in the intensities of both signals with pH may be due either to metal-NA complex formation or to direct changes in ionization efficiency due to pH.

Generally speaking, metal-NA complexes were scarcely formed at acidic pH values, partially formed around neutral values and completely formed at basic pH values, although some differences were observed among the different metal-NA complexes (Figs. 3(A)–3(F)). At pH values above 6.5 no NA signal was observed in the mass spectra, with the

exception of the cases of Mn(II) and Fe(III) (Figs. 3(A) and 3(F)). This was not due to a negative effect of high pH on the ionization efficiency of NA, which instead increased at high pH values (see Fig. II in the Supplementary Material).

With Mn(II)-NA, the signal corresponding to the complex appeared at a pH of approximately 6.2 and increased until pH 8.4 (Fig. 3(A)). In this pH range, the NA signal decreased until it was no longer observed, suggesting that at pH 8.4 all NA was present as Mn(II)-NA. With Cd(II)-NA, the signal was minor at low pH values, and increased markedly at pH values of 6.5 and above; at pH 8.0 the free NA signal was very small (Fig. III in the Supplementary Material). The signals of Fe(II)-NA and Zn(II)-NA complexes were first observed at pH values much lower than those found for Mn(II)-NA (Figs. 3(B) and 3(C)). The Fe(II)-NA and Zn(II)-NA signals sharply increased at pH values of approximately 6.2, whereas the NA signal decreased in the same pH range. At pH values above pH 6.2, metal-NA complex signal intensities did not change significantly and the NA signal was no longer observed. These data suggest that Fe(II)-NA and Zn(II)-NA complexes were completely formed at pH values of 6.2 or above. Ni(II)-NA and Cu(II)-NA signals were observed at pH values more acidic than those found for the

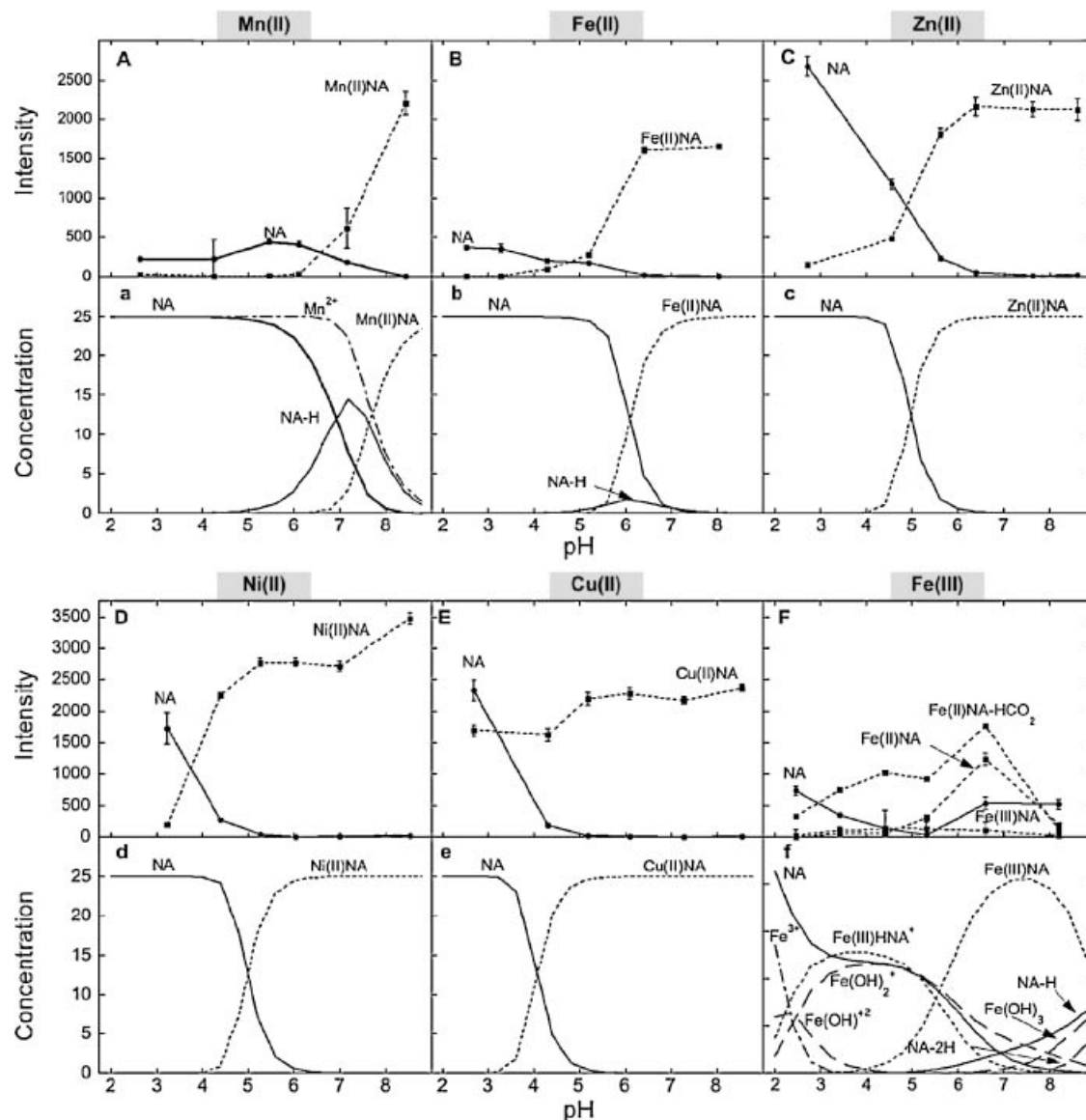


Figure 3. Software calculated (lower case letters) and experimental (upper case) pH dependences of the metal complexes of NA with Mn (A, a), Fe(II) (B, b), Zn(II) (C, c), Ni(II) (D, d), Cu(II) (E, e), and Fe(III) (F, f). Experimental values (means \pm SE, $n = 3$) show NA (solid line and circles) and metal-NA (dotted line and squares) major ion signal intensities obtained by ESI-MS analysis of a $50 \mu\text{M}$ metal complex prepared by adding equimolar amounts of nicotianamine and metal chloride solutions, either in 100 mM ammonium acetate (pHs lower than 7) or 100 mM ammonium bicarbonate (pHs higher than 7). Samples were diluted with 50% acetonitrile and pH was measured just before direct injection. *In silico* calculated values show the concentrations of the species NA (solid line) and metal-NA (dotted line) for NA and metal concentrations of $50 \mu\text{M}$. When non-coincident with NA values, the concentration of free metal is also shown as dot-line-dot curve. Fe(III) hydroxides are shown as line-space curves.

other metal-NA complexes (Figs. 3(D) and 3(E)). In the case of Cu(II)-NA, large signals were observed even at pH values lower than 3.0 (Fig. 3(E)). In both cases no signal for NA was found at pH values of 5.2 or above, suggesting that metal-NA complexes were completely formed at these pH values. A positive effect on ionization at very high pH was found only in the case of Ni(II)-NA (Fig. 3(D)).

In the case of Fe(III)-NA, a different pattern of metal-NA complex formation was found when compared with the rest of the metals (Fig. 3(F)). The NA signal disappeared at approximately pH 5.3, suggesting the total formation of the

complex, and reappeared at higher pH values. This is possibly due to the formation of deprotonated NA (both NA and deprotonated NA give the same ion in MS spectra, see below). The two daughter signals of the Fe(III)-NA metal complex also increase its intensity until pH values close to 6.2, to decrease thereafter.

These experimental results can be compared with *in silico* simulations obtained with MINTEQA2 (Figs. 3(a)–3(f)), which predict the equilibrium composition of aqueous solutions. However, some considerations should be made when comparing both approaches. First, *in silico* predictions

are always done assuming that the system has reached equilibrium, which is not likely to occur in the ESI-MS experiments. Moreover, the ESI process can induce equilibrium shifts in metal-ligand reactions.⁴³ Also, ESI-MS does not allow for the determination of some species predicted to occur by the *in silico* approach (i.e. Fe hydroxides), and some of the species predicted *in silico*, such as NA-H and NA, would give the same signal in the negative ion mode. Finally, all *in silico* predictions are done with stability and protonation constants calculated experimentally in aqueous solutions, whereas in ESI-MS experiments an organic solvent is generally needed to enhance the analyte signals, and this may affect the chemistry of the metal-NA complexes. Equilibrium constants used in the Minteqa2 thermodynamic database are determined always in water, and constants in other solvents or solvent mixtures are still rarely available due to the scarce knowledge of the physical properties of organic solvents (e.g. static dielectric constant). In recent years, the extensive use of organic solvent mixtures in chromatography has driven research in this area, and for instance static dielectric constants and density of acetonitrile mixtures at different temperatures and solvent concentrations have been only recently determined.⁴⁴

The use of both approaches led to similar conclusions, although ESI-MS data indicate that the metal-NA complexation processes do occur at lower pH values (1–2 units) than those estimated *in silico*. For instance, Mn(II)-NA shows by ESI-MS a similar behaviour to that predicted *in silico*, although the signal of the Mn(II)-NA complex appeared at a pH value almost 1 unit lower than that predicted *in silico*. The same applies for Fe(II)-NA, although in this case the difference between the *in silico* predictions and the experimental values was even larger. In the case of Zn(II)-NA, Ni(II)-NA and Cu(II)-NA, the metal-NA complexes were predicted to occur only at pH values higher than of 4.0, 4.0 and 3.0, respectively, whereas all these compounds were seen by ESI-MS at lower pH values. In the case of Fe(III), the observed increase in the signal of free NA at neutral and basic pH could be due to the occurrence of the NA-H species, also predicted to occur *in silico*, which would give in ESI-MS the same signal than NA. No software simulation could be carried out for Cd(II)-NA, because the stability constant for this complex is not available.

These results indicate that the Fe(II)-NA complex could occur at the acidic pH values usually found in the xylem of the model plant species sugar beet, around 5.5,¹⁶ conversely to what is predicted *in silico*. The Fe(III)-NA, Cu(II)-NA, Ni(II)-NA and Zn(II)-NA complexes would also occur at this pH, as seen by MS and predicted *in silico*. These data would support the role of NA in xylem transport of Fe(II), Fe(III), Cu(II), Ni(II) and Zn(II). A role for NA in the transport of Cu(II) and Ni(II) had already been proposed by other studies.^{27,41} At more neutral and alkaline pH values, corresponding to the typical pHs found in the cytosol and phloem, NA would be able to complex all metals studied.

The results also show the importance of pH when establishing extraction, separation and determination methods for metal-NA complexes. To determine what are the metal species occurring in a specific plant cell compartment, the pH of that compartment should be kept as constant

as possible throughout the whole extraction and determination processes. Lowering the pH could lead to the rupture of the metal-NA complexes, whereas using pH values significantly higher than those found in plant samples may lead to the formation of metal complexes not occurring in the sample. One example of this would be the determination of Fe-NA complexes in xylem samples with an HPLC method buffered at neutral pH, which could result in the formation of Fe(II)-NA complexes not present in the original sample.

Another issue is that organic solvent mixtures are usually employed when determining metal species with ESI-MS, and in these cases the pH values measured by using electrodes calibrated with aqueous buffers is not necessarily the true pH value. There are two possible ways of obtaining correct pH values with solvent/water mixtures. First, pH can be assessed by calibrating the pH electrode with buffers containing the organic solvent in question and then measuring the pH (${}^s\text{pH}$) in the organic solvent-containing sample. A second option is to measure pH values after electrode calibration with the aqueous buffers (${}^w\text{pH}$), and then calculate ${}^s\text{pH}$ as ${}^w\text{pH} - \theta$, with the coefficient θ being estimated by appropriate equations using the temperature value and the specific composition of the buffer (see, for instance, Eqn. (12) in Gagliardi *et al.*⁴⁵ for acetonitrile/water buffers). In our case, using 50% acetonitrile in water and at 25°C, the calculated ${}^s\text{pH}$ values would be 0.3 pH units higher than the measured ${}^w\text{pH}$ (for this particular buffer composition, θ has a negative value, see Gagliardi *et al.*⁴⁵) This indicates that only part, but not all, of the pH discrepancy in metal-NA speciation between the experimental ESI-MS data and the *in silico* calculated values could be due to this issue.

The pH difference issue should be taken into account in the development of chromatographic methods, especially if high concentrations of any organic solvent are being used. As an example, we have plotted the real pH value of the solvent mixture entering the column at different pH values in the method developed by Xuan *et al.*³⁵ (Fig. IV in the Supplementary Material). The percentage of acetonitrile at approximately 15 min (a retention time close to those of most metal complexes in that method) would be approximately 70%, leading to a θ value of approximately -0.7 units. Furthermore, the θ value at the beginning of the chromatographic run (in 90% acetonitrile) would be -1.9 pH units, so that metal complexes would be exposed to this pH value at the beginning of the chromatographic run.

Exchange reactions of Fe-NA complexes with metals and citrate

The occurrence of Fe-NA complexes in plant fluids is a key issue in order to understand Fe transport within plants. Therefore, the changes in the signals of free NA and the metal-NA complexes (Fe(II)-NA, Fe(III)-NA, Cu(II)-NA and Zn(II)-NA) with the addition of equimolar amounts of citrate, Cu or Zn, were measured. All reactions were done at two physiological relevant pH values, 5.5 as representative of xylem sap and 7.5 as representative of phloem sap.

The effect of citrate on the stability of the Fe-NA complexes was assayed at equimolar concentrations of citrate and Fe-NA. At pH 5.5, a major signal corresponding to the $[\text{M}-\text{H}]^{-1}$ ion of Fe(II)-NA can be seen in the ESI-MS spectrum

(Fig. 4(A), left panel), although minor signals for the $[M-H]^{-1}$ ion of free NA and the $[Fe(II)NA-HCO_2]^{-1}$ ion can also be observed. Once 50 μ M citrate is added, however, the Fe(II)-NA signal is reduced significantly and the free NA signal becomes approximately 4 times larger than that found in the absence of citrate (Fig. 4(A), right panel). Assuming that Fe(II)-NA solutions can contain a certain amount of Fe(III)-NA produced during preparation, ligand exchange would take place with any Fe-NA complexes and not exclusively with Fe(II)-NA. *In silico* predictions indicate that the amount of Fe(II)-NA complex in these conditions would only account for a small percentage of total Fe, 1.4%, with Fe-citrate complexes accounting for 56% of total Fe, and the rest of Fe occurring as free Fe(II). No Fe-citrate complexes were observed by ESI-MS, but free citrate did show a very large signal at m/z 191 (out of the range shown in Fig. 4). Using larger concentrations of citrate produced a major inhibition in all signals, likely due to ionization interferences. With Fe(III)-NA, significant signals of the two product ions can be seen in the ESI-MS spectrum at pH 5.5 (Fig. 4(B), left panel), although the signal for free NA can also be observed. However, once citrate was added, the Fe(III)-NA signals almost disappeared and the NA signal became much larger than in the absence of citrate (Fig. 4(B), right panel). Therefore, Fe(III)-NA seems to be more sensitive than Fe(II)-NA to the presence of citrate. Conversely, *in silico* predictions indicate that the amount of Fe(III) chelated by NA would be 33% of the total, with Fe-citrate complexes accounting for 56% of the total Fe, the rest of Fe occurring as Fe hydroxide. These results would support the current view that in the xylem, where quite large concentrations of citrate are usually present (up to the mM range),¹⁶ Fe-citrate complexes would be the major Fe species.^{3,16} At pH 7.5, a large signal of the Fe(II)-NA complex can be seen in the ESI-MS spectrum (Fig. 4(C), left panel), and no signal for free NA was observed. When citrate was added, the Fe(II)-NA complex signal was reduced but no signal of the free NA at

m/z 302 was observed (Fig. 4(C), right panel), suggesting that at this pH the Fe(II)-NA complex is still stable in the presence of 50 μ M citrate. Citrate ionization could negatively affect Fe(II)-NA and NA ionization, resulting in decreases in the intensities of the $[NA-H]^{-1}$ and $[Fe(II)NA-H]^{-1}$ ion signals. *In silico* predictions also indicate that the amount of Fe(II)-NA complex in these conditions would account for 94% of total Fe, with Fe-citrate complexes accounting for only 6% of total Fe. At pH 7.5, significant signals of the two product ions of the Fe(III)-NA complex were seen in the ESI-MS spectrum (Fig. 4(D), left panel), and the signal for free NA was also observed. Once citrate was added, one of the product ion signals (the $[Fe(II)NA-HCO_2]^{-1}$ ion) almost disappeared, whereas the other did not change much and the NA signal did not increase (Fig. 4(D), right panel). This indicates that the Fe(III)-NA complex is less affected by citrate at pH 7.5 than at pH 5.5. *In silico* predictions indicated that the amount of Fe(III) chelated by NA would be 82% of the total, with Fe-citrate complexes being practically absent. It should be taken into account that the citrate/Fe ratios in sap could be much higher than 1:1 (in some cases as high as 2000:1),⁴⁶ and therefore the real effects of citrate could be much more extreme than those found here.

Metal-exchange reactions between Fe(II)-NA, Zn(II) and Cu(II) were also studied. At pH 5.5, the only major signal found with Fe(II)-NA was the one corresponding to the $[M-H]^{-1}$ ion (Fig. 5(A), left panel). After addition of Zn(II), a good signal for the Zn(II)-NA complex was observed, whereas the signal of the Fe(II)-NA complex was reduced to values lower than that of Zn(II)-NA (Fig. 5(A), right panel), indicating a rapid metal exchange in agreement with the stability constant values of these complexes (15.4 for Zn(II) and 12.8 for Fe(II)). At pH 7.5 (Fig. 5(B)) the Fe(II)-NA complex seems to be quite stable in the presence of Zn(II), since only a small signal for the Zn(II)-NA complex was observed while the Fe(II)-NA signal was little decreased. *In silico* predictions, however, indicate that most of the NA

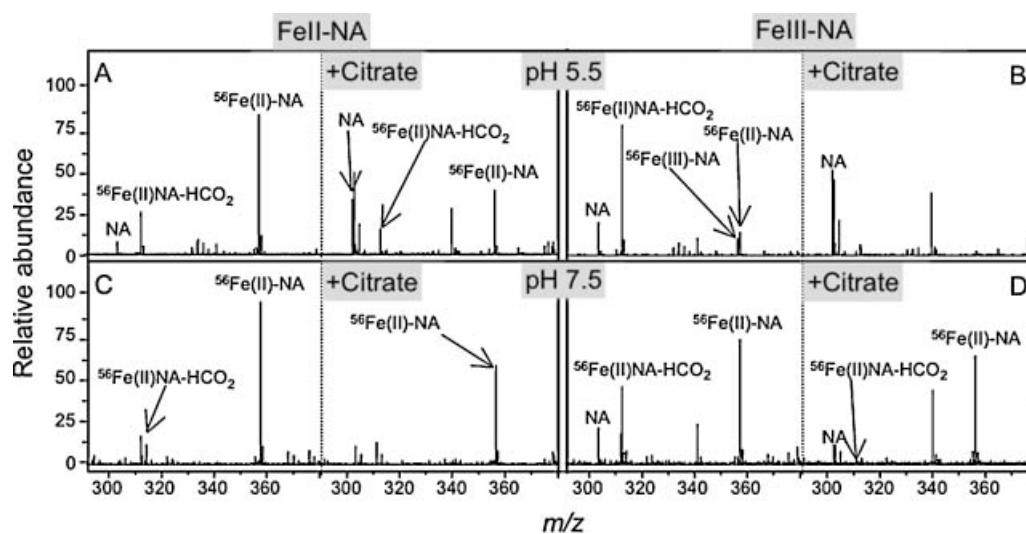


Figure 4. Ligand-exchange reactions between Fe(II)-NA and citrate at pH 5.5 (A) and pH 7.5 (C), and between Fe(III)-NA and citrate at pH 5.5 (B) and pH 7.5 (D). Citrate and Fe-NA complex concentrations of the initial solutions were 50 μ M. Solutions were prepared in 100 mM ammonium acetate (pH 5.5) or ammonium bicarbonate (pH 7.5) and 50% acetonitrile.

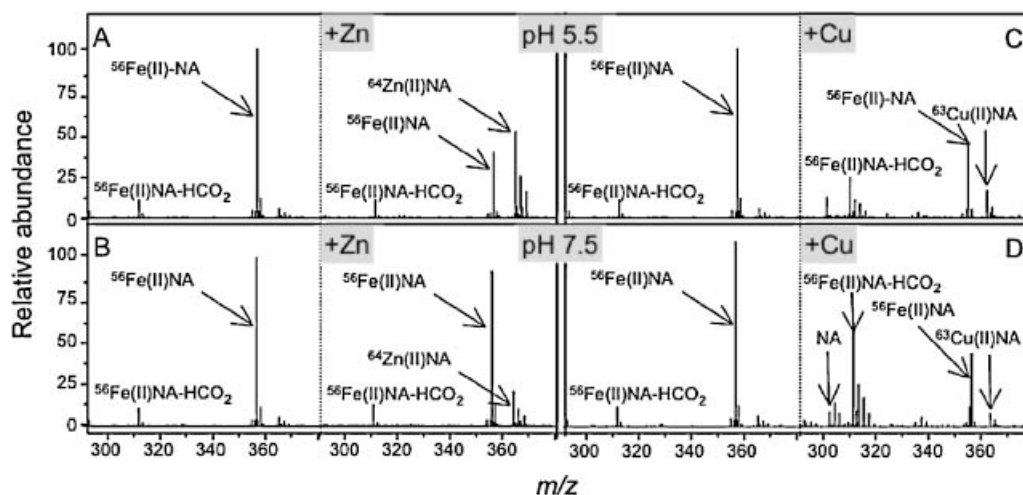


Figure 5. Metal-exchange reactions between Fe(II)-NA and Zn(II) at pH 5.5 (A) and pH 7.5 (B), and between Fe(II)-NA and Cu(II) at pH 5.5 (C) and 7.5 (D). Metal and Fe(II)-NA complex concentrations of the initial solutions were 50 μ M.

should be chelating Zn(II) at both pH values. Possibly, the discrepancies between the observed speciation and the *in silico* predictions could be due to the kinetics of the exchange reaction. At pH 5.5, after the addition of Cu(II) to the Fe(II)-NA solution there was a large decrease of the Fe(II)-NA signal, although the signal of Cu(II)-NA was not very large (Fig. 5(C)). This supports the existence of metal exchange, as it could be expected from the values of the stability constants. The low intensity of the Cu(II)-NA complex can be explained by the voltage value used in the experiment (120 V), since the optimal voltage value found for the Cu(II) complex was 90V (Fig. I in the Supplementary Material). Also, signals for free NA and the $[M-H-CO_2]^{-1}$ ion of Fe(II)-NA were observed. At pH 7.5 a similar behaviour was observed, although the peak at m/z 311 corresponding to the $[Fe(II)NA-H-CO_2]^{-1}$ ion was larger than at pH 5.5 (Fig. 5(D)). *In silico* predictions indicate that most of the NA should be chelating Cu(II) at both pH values.

CONCLUSIONS

Results indicate that relatively small changes in pH and changes in the concentrations of citrate and metals can have significant effects in NA speciation in plant fluids such as xylem and phloem sap. In the xylem sap, NA is not likely to complex Fe due to exchange reactions with citrate and other metals, whereas it could chelate other metals such as Cu and Ni. In the phloem sap, NA could still be a good candidate to chelate Fe, specially in the Fe(II) form. Some metal-NA complexes, including Fe(II)-NA and Fe(III)-NA, were found by ESI-MS at lower pH values than those estimated *in silico*, and this effect could be only partially explained by the estimated size of the errors associated to measuring pH in organic-solvent-containing solutions. Our work and recent examples of other researchers have shown the feasibility of ESI-MS to study metal-NA complexes within plant fluids, but some drawbacks inherent to the technique need to be addressed: namely, the need to maintain as much as possible the pH of the plant compartment under study through the whole extraction, separation and analysis process, the

possible changes in metal-ligand complex chemistry and the difficulty to assess the true pH value in solutions with a considerable amount of organic solvent, and the possibility that metal redox reactions may occur in the ESI process. Our work has also shown that *in silico* predictions may fail to accurately speciate NA in non-equilibrium solutions such as plant fluids. It should also be mentioned that in real plant samples other metals such as Ca and ligands such as glutathione may affect the interpretations proposed here. However, it would be unrealistic to analyze plant fluids by direct infusion ESI-MS due to matrix effects. To avoid matrix interferences a previous separation technique such as liquid chromatography is mandatory.³⁶ Direct determination of metal-NA complexes in plant fluids may change the current knowledge on the role of NA in micronutrient plant nutrition.

SUPPLEMENTARY MATERIAL

The supplementary electronic material for this paper is available in Wiley InterScience at: <http://www.interscience.wiley.com/jpages/0951-4198/suppmat/>.

Acknowledgements

This work was supported by the Spanish Ministry of Science and Education (Grant Nos. AGL2006-1416 and AGL2007-61948, co-financed with FEDER), the European Commission (EU 6th Framework Integrated Project ISA-FRUIT), and the Aragón Government (group A03). The authors would also like to thank the two reviewers for helpful contributions.

REFERENCES

- Hall JL. *J. Exp. Bot.* 2002; **53**: 1. DOI: 10.1093/jexbot/53.366.1.
- Noma M, Noguchi M, Tamaki E. *Tetrahedron Lett.* 1971; 2017.
- von Wirén N, Klair S, Bansal S, Briat JF, Khodr H, Shioiri T, Leigh RA, Hider RC. *Plant Physiol.* 1999; **119**: 1107.
- Benes I, Schreiber K, Ripberger H, Kircheiss A. *Experientia* 1983; **39**: 261.
- Stephan UW, Scholz G. *Physiol. Plant.* 1993; **88**: 522.

6. Anderegg G, Ripperger H. *J. Chem. Soc.-Chem. Commun.* 1989; **647**: DOI: 10.1039/C39890000647.
7. Hell R, Stephan UW. *Planta* 2003; **216**: 541. DOI: 10.1007/s00425-002-0920-4.
8. Stephan UW, Schmidke I, Stephan VW, Scholz G. *Biometals* 1996; **9**: 84. DOI: 10.1007/BF00188095.
9. Scholz G, Becker R, Pich A, Stephan UW. *J. Plant Nutr.* 1992; **15**: 1647.
10. Stephan UW, Scholz G. *J. Plant Physiol.* 1990; **136**: 631.
11. Herbig A, Giritch A, Horstmann C, Becker R, Balzer HJ, Baumlein H, Stephan UW. *Plant Physiol.* 1996; **111**: 533.
12. Liu DH, Adler K, Stephan UW. *Protoplasma* 1998; **201**: 213. DOI: 10.1007/BF01287417.
13. Takahashi M, Terada Y, Nakai I, Nakanishi H, Yoshimura E, Mori S, Nishizawa NK. *Plant Cell* 2003; **15**: 1263. DOI: 10.1105/tpc.010256.
14. Pich A, Scholz G, Stephan UW. *Plant Soil* 1994; **165**: 189. DOI: 10.1007/BF00008061.
15. Tiffin LO. *Plant Physiol.* 1966; **41**: 510.
16. Lopez-Millan AF, Morales F, Abadía A, Abadía J. *Plant Physiol.* 2000; **124**: 873.
17. Durrett TP, Gassmann W, Rogers EE. *Plant Physiol.* 2007; **144**: 197. DOI: 10.1104/pp.107.097162.
18. Schmidke I, Kruger C, Frommichen R, Scholz G, Stephan UW. *Physiol. Plant.* 1999; **106**: 82.
19. Kruger C, Berkowitz O, Stephan UW, Hell R. *J. Biol. Chem.* 2002; **277**: 25062. DOI: 10.1074/jbc.M201896200.
20. Maas FM, Vandewetering DAM, Vanbeusichem ML, Bienfait HF. *Plant Physiol.* 1988; **87**: 167.
21. Herbig A, Koch G, Mock HP, Dushkov D, Czihal A, Thielmann J, Stephan UW, Baumlein H. *Eur. J. Biochem.* 1999; **265**: 231.
22. Higuchi K, Suzuki K, Nakanishi H, Yamaguchi H, Nishizawa NK, Mori S. *Plant Physiol.* 1999; **119**: 471.
23. Ling HQ, Koch G, Baumlein H, Ganai MW. *Proc. Natl. Acad. Sci. USA* 1999; **96**: 7098.
24. Koike S, Inoue H, Mizuno D, Takahashi M, Nakanishi H, Mori S, Nishizawa NK. *Plant J.* 2004; **39**: 415. DOI: 10.1111/j.1365-313X.2004.02146.x.
25. Roberts LA, Pierson AJ, Panaviene Z, Walker EL. *Plant Physiol.* 2004; **135**: 112. DOI: 10.1104/pp.103.037572.
26. Schaaf G, Schikora A, Haberle J, Vert G, Ludewig U, Briat JF, Curie C, von Wiren N. *Plant Cell Physiol.* 2005; **46**: 762. DOI: 10.1093/pcp/pci081.
27. Pich A, Scholz G. *J. Exp. Bot.* 1996; **47**: 41.
28. Vacchina V, Mari S, Czernic P, Marques L, Pianelli K, Schaumloffel D, Lebrun M, Lobinski R. *Anal. Chem.* 2003; **75**: 2740. DOI: 10.1021/ac020704m.
29. Weber M, Harada E, Vess C, von Roepenack-Lahaye E, Clemens S. *Plant J.* 2004; **37**: 269. DOI: 10.1046/j.1365-313X.2003.01960.x.
30. Kim S, Takahashi M, Higuchi K, Tsunoda K, Nakanishi H, Yoshimura E, Mori S, Nishizawa NK. *Plant Cell Physiol.* 2005; **46**: 1809. DOI: 10.1093/pcp/pci196.
31. Douchkov D, Gryczka C, Stephan UW, Hell R, Baumlein H. *Plant Cell Environ.* 2005; **28**: 365.
32. Pianelli K, Mari S, Marques L, Lebrun M, Czernic P. *Transgenic Res.* 2005; **14**: 739. DOI: 10.1007/s11248-005-7159-3.
33. Hider RC, Yoshimura E, Khodr H, von Wiren N. *New Phytol.* 2004; **164**: 204. DOI: 10.1111/j.1469-8137.2004.01209.x.
34. Ouerdane L, Mari S, Czernic P, Lebrun M, Lobinski R. *J. Anal. At. Spectrom.* 2006; **21**: 676. DOI: 10.1039/b602689c.
35. Xuan Y, Scheuermann EB, Meda AR, Hayen H, von Wiren N, Weber G. *J. Chromatogr. A* 2006; **1136**: 73.
36. Weber G, von Wiren N, Hayen H. *Rapid Commun. Mass Spectrom.* 2006; **20**: 973. DOI: 10.1002/rcm.2402.
37. Martell AE, Smith RM. *Critical Stability Constants*. Plenum: New York, 1974.
38. Neubert H, Hider RC, Cowan DA. *Rapid Commun. Mass Spectrom.* 2002; **16**: 1556. DOI: 10.1002/rcm.756.
39. Blades AT, Ikonomou MG, Kebarle P. *Anal. Chem.* 1991; **63**: 2109.
40. Pecoraro V, Bonadies JA, Marrese CA, Carrano CJ. *J. Am. Chem. Soc.* 1984; **106**: 3360.
41. Mari S, Gendre D, Pianelli K, Ouerdane L, Lobinski R, Briat JF, Lebrun M, Czernic P. *J. Exp. Bot.* 2006; **57**: 4111. DOI: 10.1093/jxb/erl184.
42. Schaumloffel D, Ouerdane L, Bouyssiere B, Lobinski R. *J. Anal. At. Spectrom.* 2003; **18**: 120.
43. Wang HJ, Agnes GR. *Anal. Chem.* 1999; **71**: 4166. DOI: 10.1021/ac981375u.
44. Gagliardi LG, Castells CB, Rafols C, Roses M, Bosch E. *Journal of Chemical and Engineering Data* 2007; **52**: 1103. DOI: 10.1021/je700055p.
45. Gagliardi LG, Castells CB, Rafols C, Roses M, Bosch E. *Anal. Chem.* 2007; **79**: 3180. DOI: 10.1021/ac062372h.
46. Abadía J, Lopez-Millan A, Rombola A, Abadía A. *Plant and Soil* 2002; **241**: 75.